
This is an electronic reprint of the original article.
This reprint may differ from the original in pagination and typographic detail.

Goel, Priyanka; Tittonen, Ilkka; Raju, Ramesh; Koskinen, Tomi; Kornienko, Vladimir;
Wojnicka, Weronika

Thermoelectric and Optical Properties of Nanostructured p-Type CuI Thin Films Grown by Glancing Angle Deposition for Transparent Energy-Harvesting Applications

Published in:
ACS Applied Nano Materials

DOI:
[10.1021/acsanm.4c06004](https://doi.org/10.1021/acsanm.4c06004)

Published: 27/12/2024

Document Version
Publisher's PDF, also known as Version of record

Published under the following license:
CC BY

Please cite the original version:
Goel, P., Tittonen, I., Raju, R., Koskinen, T., Kornienko, V., & Wojnicka, W. (2024). Thermoelectric and Optical Properties of Nanostructured p-Type CuI Thin Films Grown by Glancing Angle Deposition for Transparent Energy-Harvesting Applications. *ACS Applied Nano Materials*, 7(24), 28736-28742.
<https://doi.org/10.1021/acsanm.4c06004>

This material is protected by copyright and other intellectual property rights, and duplication or sale of all or part of any of the repository collections is not permitted, except that material may be duplicated by you for your research use or educational purposes in electronic or print form. You must obtain permission for any other use. Electronic or print copies may not be offered, whether for sale or otherwise to anyone who is not an authorised user.

Thermoelectric and Optical Properties of Nanostructured p-Type CuI Thin Films Grown by Glancing Angle Deposition for Transparent Energy-Harvesting Applications

Priyanka Goel,* Tomi Koskinen, Ramesh Raju, Vladimir V. Kornienko, Weronika Wojnicka, and Ilkka Tittonen



Cite This: *ACS Appl. Nano Mater.* 2024, 7, 28736–28742



Read Online

ACCESS |



Metrics & More



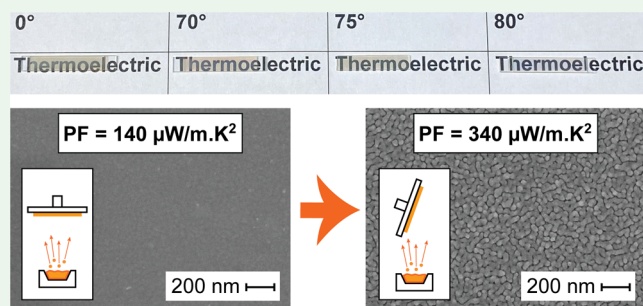
Article Recommendations



Supporting Information

ABSTRACT: Copper iodide (CuI) is recognized as a promising p-type transparent material with excellent thermoelectric properties. CuI thin films are typically produced by depositing a copper layer, followed by iodination. However, this process poses challenges in controlling the film's structure, often leading to excessive grain growth in CuI and reduced optical clarity due to increased light scattering from larger grains. In our study, we introduce an innovative method to regulate the structural characteristics of CuI films by employing the glancing angle deposition (GLAD) technique in depositing the initial copper layer. This method creates nanostructured copper films that guide the formation of CuI grains during vapor iodination. By varying the deposition angle and iodination time, we adjust the size and shape of the synthesized CuI nanostructure-sized grains. This directly enhances the thermoelectric properties and the transmittance of the CuI films. We observe that our CuI films result in a 43% increase in Seebeck coefficient (S) of $352 \mu\text{V}/\text{K}$, leading to a 90% enhancement at room temperature with a power factor of $339 \mu\text{W}/\text{mK}^2$ compared to the previously reported CuI prepared by the vapor iodination method. Additionally, these nanostructured films exhibit high transparency with a transmittance of 85% at a 560 nm wavelength, demonstrating superior optical properties at this wavelength. These results highlight the potential for integrating nanostructured p-type transparent materials into smart windows and cooling systems for optical chips.

KEYWORDS: copper iodide, glancing angle deposition, vapor iodination, thermoelectric, transparent



1. INTRODUCTION

In recent years, the study on the zinc blende phase of CuI (γ -CuI) has gained interest as a transparent p-type thermoelectric material.^{1–5} P-type thermoelectric materials are crucial for efficient thermoelectric devices as they complement transparent n-type materials like ITO,⁶ in creating thermoelectric modules that can convert heat into electricity. While there has been significant progress in using ITO, there is a notable lack of a high-performance transparent p-type thermoelectric counter material in thermoelectric generators. This gap limits the development of advanced applications like transparent electronics, smart windows, and on-chip cooling systems, making the discovery of transparent p-type materials crucial for future technologies.¹² More specifically, the γ -phase of CuI is dominant at room temperature^{3,7} and can be produced by employing physical vapor deposition (PVD) methods.^{1,4,5} The first thin film of CuI as a transparent conductive material was reported in 1907 by Bädeker after exposing Cu thin film to iodine via the vaporization method.⁸ Since then, various techniques have been incorporated for producing CuI thin films from Cu, followed by iodination through solid, liquid, or

vapor phases.^{9–11} Depending on the fabrication technique, only the submicron CuI films show enhanced transparency¹² and thermoelectric properties. The iodination process, central to CuI synthesis, involves the chemical reaction between copper and iodine, described as



In this reaction, the copper metal reacts with iodine vapor to form copper iodide (CuI), which crystallizes in the zinc blende (γ -phase) structure, which is stable at room temperature. Vapor iodination allows for efficient conversion of Cu to CuI, yielding thin films with high transparency and p-type conductivity. Effective thermoelectric materials are anticipated to exhibit a high power factor^{13–15} $\text{PF} = S^2 \sigma$, where S is the

Received: October 24, 2024
Revised: December 9, 2024
Accepted: December 10, 2024
Published: December 17, 2024



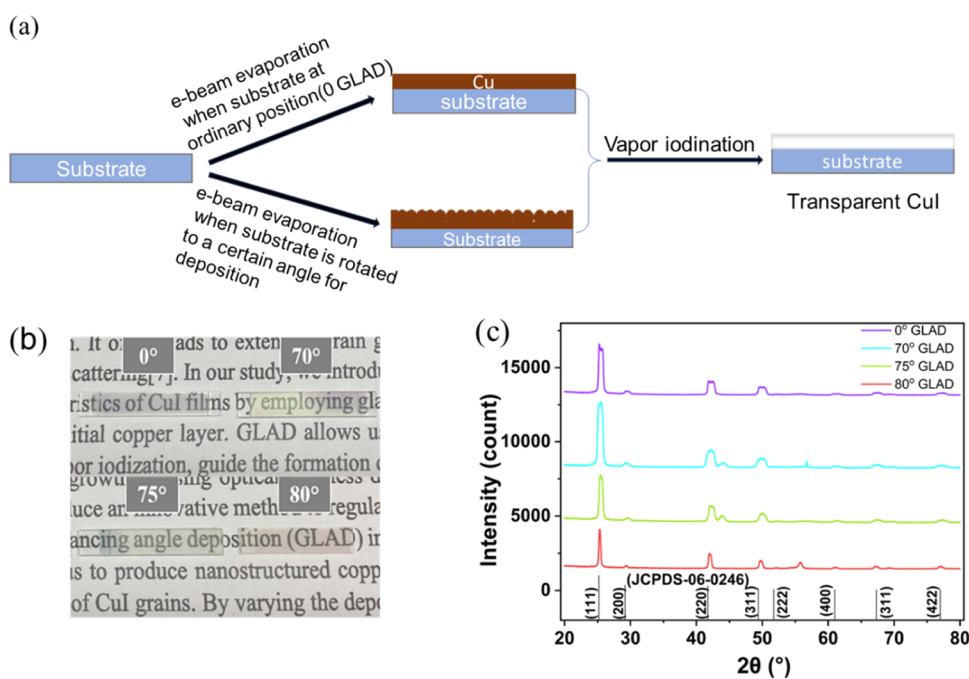


Figure 1. (a) Fabrication process of CuI thin film using the GLAD, (b) photograph showing the transparent thin film at different GLADs, and (c) GIXRD spectra of CuI thin films grown by the vapor method at different GLADs.

Seebeck coefficient and σ is the electrical conductivity. Thus, a good thermoelectric material should possess both high S and high σ . The highest S reported for CuI is $308 \mu\text{V}/\text{K}$ with a corresponding PF of $0.17 \mu\text{W}/\text{m}\cdot\text{K}^2$.¹⁶ The PF from liquid and vapor iodinations is reported as $170 \mu\text{W}/\text{m}\cdot\text{K}^2$,¹⁷ and $13 \mu\text{W}/\text{m}\cdot\text{K}^2$ ¹⁸ respectively, while the solid iodination resulted in a notably high PF of $470 \mu\text{W}/\text{m}\cdot\text{K}^2$ ²⁵ but suffered from scalability challenges. The thermoelectric performance along with high transmittance can be optimized by controlling the nanoscale structural features, particularly by adjusting the grain size. Smaller grains increase the number of grain boundaries, which enhances phonon scattering.¹⁹ This improved scattering helps maintain a high Seebeck coefficient by reducing heat loss, thereby leading to an increased power factor. Fine-tuning the grain size at the nanoscale thus becomes essential for tailoring the thermoelectric behavior, emphasizing the multifaceted nature of factors influencing the overall performance of these films. Glancing angle deposition (GLAD) is particularly effective in achieving smaller grain sizes due to the shadowing effect, which limits lateral growth and produces nanostructured films with more uniform and compact grains.^{20–23}

In addition to the thermoelectric properties, the nanoscale grain structure of CuI films significantly impacts their optical performance. Previous studies have reported lower optical performance^{17,18} due to haziness caused by extensive grain growth and thickness²⁴ of CuI during prolonged iodination from 30 min to 2 h as observed by Herrick in 1963.²⁵ On the contrary, reaction times enable the fabrication of films with optical properties close to those obtained via the solid iodination route,⁵ but at the cost of limited control over the iodine content in the film. Nevertheless, iodine-rich reaction conditions are preferred to ensure an adequate supply of iodine, which reduces iodine vacancies and defects in CuI crystals.^{18,26} This results in high-quality films with an improved performance.

In this study, we introduce the GLAD technique to investigate the thermoelectric and optical properties of CuI thin films. The nanostructured Cu films, formed through GLAD, guide the formation of the CuI films upon iodination by limiting grain growth and tailoring nanoscale features. We obtain a significantly high Seebeck coefficient of $352 \mu\text{V}/\text{K}$ and a correspondingly high power factor as a function of increasing glancing angle for Cu deposition. The resulting films are more transparent than those reported earlier.¹ The transmittance maximum due to thin film interference is shown to vary between 75 and 90% in the wavelength region of 500–900 nm, highlighting their potential for advanced transparent thermoelectric applications.

2. MATERIALS AND METHODS

2.1. Sample Preparation. CuI samples were prepared by depositing Cu thin film onto soda-lime glass substrates of sizes $4 \text{ mm} \times 20 \text{ mm}$ and $10 \text{ mm} \times 10 \text{ mm}$ using electron beam-assisted (EBA) evaporation (Angstrom Engineering) from the Cu target (99% purity). To ensure cleanliness, all substrates underwent ultrasonic cleaning with acetone, isopropyl alcohol (IPA), and deionized water (DIW) for 5 min at room temperature, followed by drying under N_2 flow. The deposition of the Cu thin film was carried out in a vacuum ranging between 10^{-6} and 10^{-7} Torr. The evaporation was conducted at a deposition rate of $0.2 \text{ nm}/\text{s}$. The target thickness of Cu film was fixed at 200 nm with the variation in glancing angle deposition (GLAD) of 0, 70, 75, and 80° for the substrates concerning the target in the deposition chamber. Also, to compete with the actual thickness of Cu deposited at 70, 75, and 80° GLAD, 50 nm Cu was deposited at 0° GLAD. The substrate-carrying stage was rotated at a speed of 20 rpm to improve the uniformity of the film.

After that, 4 g of iodine crystals were heated in a corked glass flask to 130°C for 4 min to obtain a sufficient amount of iodine vapors. Next, as-deposited copper substrates were simultaneously placed inside this flask for 30, 60, and 120 s on a three-dimensional (3D)-printed stage specifically designed for this experiment. Lastly, CuI thin films were washed with IPA immediately after iodination to remove individual iodine particles deposited from hot iodine gas condensing on the cold corner spots of the substrate. Finally, electrical contact

pads of Ti/Au (5/40 nm) were deposited using EBA, maintaining the rest of the parameters the same as used for the Cu deposition.

2.2. Structural Characterization. The thickness of the Cu and CuI films was measured using a profilometer (Dektak/XT). The crystallographic analysis of CuI thin films was conducted with grazing incidence X-ray diffractometry (GIXRD) on a Rigaku Smartlab diffractometer using copper $K\alpha$ radiation ($\lambda = 1.5418 \text{ \AA}$). XRD patterns were collected over a 2θ range of $20\text{--}80^\circ$. The surface morphology of the films was studied by a scanning electron microscope (SEM EBL Zeiss Supra 40), and the grain size of the CuI crystals was measured by analyzing SEM images using ImageJ software (details are shared in the Supporting Information). Sample surfaces were further scanned for measuring the roughness of the films by atomic force microscopy (AFM, Bruker Dimension Icon). The transmittance spectra were recorded in the visible range of $400\text{--}900 \text{ nm}$ under normal incidence using a custom-made setup based on a halogen lamp and a spectrometer (OceanOptics Flame-S-ultra-violet-visible (UV-vis)). The beam diameter of the sample was 1 mm . The Seebeck coefficient and the in-plane resistivity were measured for CuI thin films under a He atmosphere on an LSR-3 (Linseis) system with five temperature gradients with 10 min stabilization time for each gradient. The LSR-3 measurement details and the comprehensive analysis of the film properties are thoroughly discussed in a previous study.²⁷ Lastly, the Hall mobility (μ) of the samples was obtained from $10 \times 10 \text{ mm}^2$ with electrical contacts using the Hall Measurement System (HMS-5300 Ecopia) in a Van der Pauw configuration. All of the measurements were conducted at room temperature.

3. RESULTS AND DISCUSSION

3.1. Structural and Morphological Properties. The measured film thickness of as-deposited Cu (with fixed nominal thickness of 200 nm) at $0, 70, 75,$ and 80° GLAD was $167, 57, 48,$ and 34 nm , respectively. The fabrication process for CuI films is shown in Figure 1. The film thickness decreases with an increase in the deposition angle. This is because the sensor in the evaporation system has been calibrated for the substrate stage at a 0° angle. The corresponding CuI film thickness (for nominal 200 nm) at $0, 70, 75,$ and 80° GLAD after 2 min long iodination was observed to be $1.01 \mu\text{m}, 288, 260,$ and 135 nm , respectively. To compete with the thickness of the as-deposited Cu thin film, a nominal thickness of 50 nm was chosen for the 0° GLAD instead of 200 nm , as its actual thickness corresponds more closely to the actual thickness of the other three samples at $70, 75,$ and 80° with a nominal thickness of 200 nm reported in Table 1. The thicknesses of all other samples prepared at the 30 and 60 s were also measured and are reported in S1–S4.

Insight into the crystalline structure of the films was obtained through GIXRD measurements. The crystallography of CuI thin films obtained at different GLADs is shown in Figure 1. The diffraction peaks that were obtained at $25.5, 29, 42.5, 50, 67,$ and 76° confirm the polycrystalline nature of all of the CuI thin films.^{18,28} The maximum intensity peak

takes place at 25.5° indicating that the film growth is directed along the (111) plane. The sharpest peaks are observed at 80° GLAD grown films as seen in Figure 1c. This confirms the presence of well-defined crystallographic planes within this crystalline CuI. The diffractographs match JCPDS-06-0246 for the Zinc blend structure of the γ -CuI phase.^{7,29,30} The average crystallite size (D) is calculated using the Debye–Scherrer equation³¹

$$D = \frac{0.9\lambda}{\beta \cos \theta} \quad (2)$$

where $\beta = \text{fwhm}$ (in radians), $\theta = \text{peak position}$ (in radians), and $\lambda = 1.5418 \text{ \AA}$. The average crystallite size (calculated from XRD pattern) is found to be 24 nm for 2 min iodination at 80° GLAD, which is smaller than the average grain size determined by SEM (crystallite sizes of other samples are reported in S5). This indicates that multiple similarly oriented crystallites agglomerated³¹ to form larger CuI grains as observed in the SEM images (Figure 2). The surface view SEM images of as-deposited Cu films at different angles reveal variations in the granular structure as a function of GLAD, as shown in Figure 2(a–d). These structural changes in as-deposited Cu films subsequently influence the formation of CuI in the resulting thin films, as can be seen in Figure 2e–2h. At 0° GLAD, Cu is deposited more uniformly, leading to a denser film with almost zero voids, as seen in Figure 2a. At higher angles, the film tends to be more porous, as observed in Figure 2b–d. This increased porosity is linked to a decrease in the film's overall density, as a film with less material is packed into the same volume. This effect occurs because the shadowing effect becomes more pronounced at higher angles.³² It appears that the porous structure provided a larger surface area and more nucleation sites for the iodination reaction, which might have encouraged the growth of smaller CuI grains at different GLADs. It also shows the random distribution and orientation of faceted crystals composed of diverse sizes in the range from 85 to 270 nm . The average grain sizes after 2 min iodination are measured from SEM micrographs using ImageJ software being reported in Table 1. The average grain size of $121 \pm 13 \text{ nm}$ was observed in 80° GLAD CuI nanostructured film which is 35% smaller than the grain size of 186 nm reported by Faustino et al.⁵

Topography of the films was observed using AFM, and RMS roughness values were measured for CuI thin films at $0, 70, 75,$ and 80° GLAD as $11.3, 16, 11.6,$ and 9.3 nm , respectively. Despite the presence of grains of varying sizes, the overall height variations across the surface average to a low value, as indicated by the RMS roughness. This measurement reflects the overall smoothness of the film surface. Consequently, the RMS roughness values suggest that variations in the surface texture and uniformity at different orientations could influence the film's optical and thermoelectric properties. The topographical data with its 3D representation within CuI films can be seen in S9 of the Supporting Information.

3.2. Thermoelectric Properties. Seebeck coefficient and charge carrier concentrations are obtained as positive, which confirms the p-type semiconductor behavior of the fabricated CuI films. The p-type nature is because of Cu vacancies (V_{Cu}) that have been reported as the main acceptors in p-type CuI ($V_{\text{Cu}} \rightarrow V_{\text{Cu}}^- + h^+$).⁹ The highest Seebeck coefficient of $352 \mu\text{V/K}$ and a power factor of $3.39 \times 10^{-4} \text{ W/mK}^2$ are measured in CuI films where Cu is deposited at 80° GLAD for 2 min of iodine exposure. The results are shown in Figure 3

Table 1. Actual Thickness of As-Deposited Cu, CuI Thin Films, and the Average Grain Size Measured at Different GLADs of $0, 70, 75,$ and 80°

GLAD	thickness (nm) Cu film	thickness (nm) CuI film	average grain size (nm) of a CuI grain on the surface
0°	41 ± 3	213.7 ± 4	247 ± 9
70°	57 ± 0.6	288 ± 2	173 ± 9
75°	48 ± 0.2	260 ± 1	164 ± 15
80°	34 ± 0.4	135 ± 2	121 ± 13 (very small)

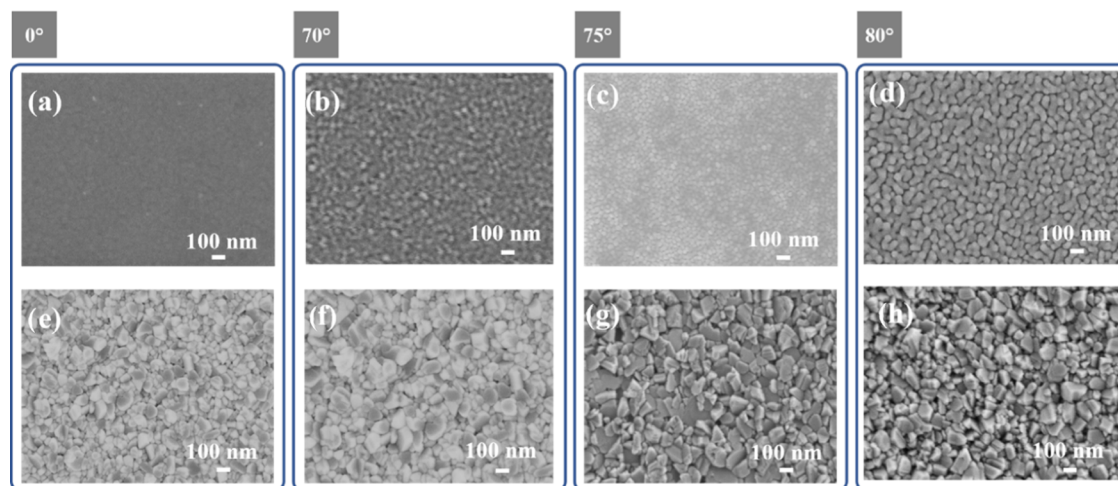


Figure 2. Top-view SEM images of as-deposited Cu (a–d) and corresponding CuI (e–h) thin films prepared at 0, 70, 75, and 80° GLAD with a 2 min I_2 exposure time.

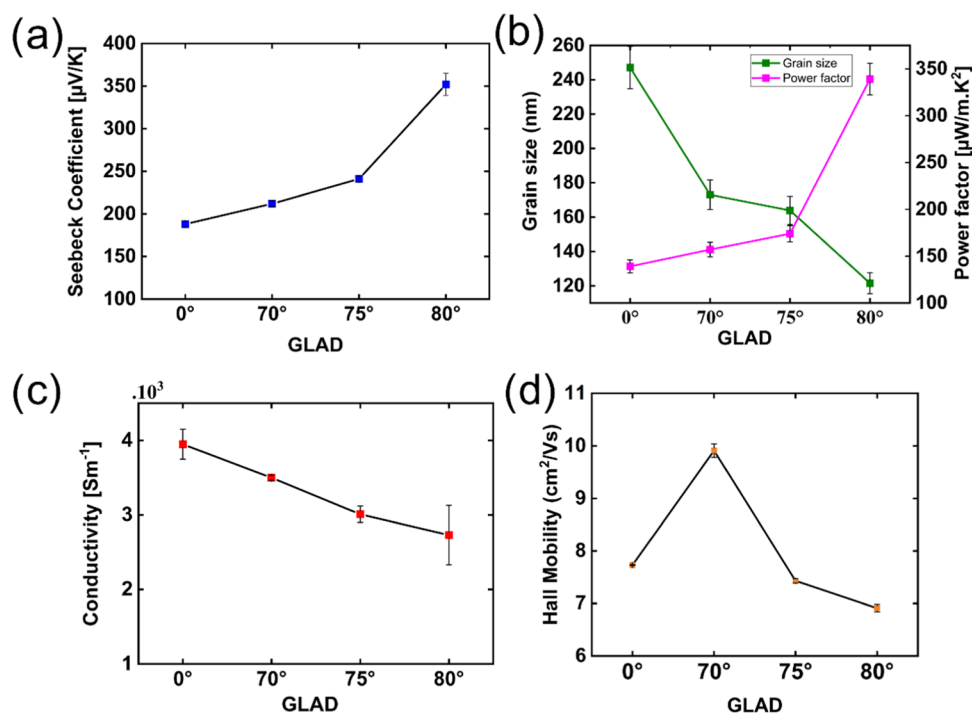


Figure 3. Thermoelectric and electronic transport performance of CuI thin films: (a) Seebeck coefficient; (b) power factor and grain size; (c) electrical conductivity; (d) hall mobility; the error bars in the graph represent the standard deviation from three sample measurements. For the Hall measurements, some of the error bars are smaller than the data points in the graphs.

including the Seebeck coefficient (3a), power factor (3b), and electrical conductivity (3c). These values are higher than the previously reported values.^{5,7,18,33} The Seebeck coefficient and other electrical properties of CuI as a function of iodination time (30 and 60 s iodine exposure) can be found in S6. The enhancement of thermoelectric properties can be attributed to the smaller grain size as compared to previous work.^{5,18} As the grain size decreases, the mean free path of the carriers decreases, leading to increased scattering.³⁴ This results in a higher Seebeck coefficient, which in turn contributes to an enhancement in the power factor, as illustrated in Figure 3b. Additionally, enhancement in Seebeck coefficients can be due to improved crystallinity.³⁵ However, the electrical conductivity of the CuI films decreases as the GLAD increases from 0 to

80°. The decrease in electrical conductivity as the GLAD increases from 0 to 80° is primarily due to the reduction in grain size, which increases the density of grain boundaries. These grain boundaries act as scattering centers for charge carriers, impeding their transport³⁶ and thereby lowering the electrical conductivity.

We gain insight into the electronic properties of the films through Hall mobility measurements conducted using the van der Pauw geometry. These results are presented in Figure 3d. The hole mobility observed is lower than what was previously reported.⁵ This indicates as the grain size reduces with the GLAD technique, more grain boundaries have emerged, as evident in the SEM images. These grain boundaries cause significant scattering of the carriers, thereby reducing the

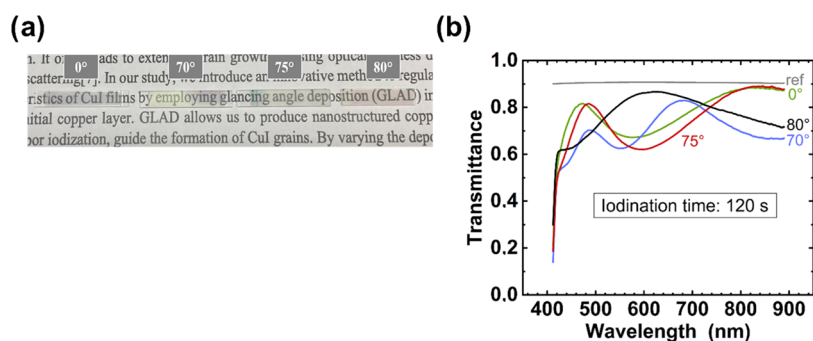


Figure 4. Optical properties of CuI films deposited from 120 s iodine exposure at 0, 70, 75, and 80° GLAD. (a) Picture illustrating the difference in optical transparency of CuI films deposited with different GLADs on soda-lime glass. (b) Transmittance spectra of the same samples.

charge carrier mobility. The reduction in carrier mobility from $7.71 \text{ cm}^2 \text{ V}^{-1} \text{ s}^{-1}$ at 0° GLAD to $6.9 \text{ cm}^2 \text{ V}^{-1} \text{ s}^{-1}$ at 80° GLAD due to enhanced scattering typically results in reduced electrical conductivity as shown in Figure 3c. However, if the grain boundaries primarily scatter low-energy carriers and allow high-energy carriers to move more freely, the Seebeck coefficient can still increase because it reflects the contribution of these higher-energy carriers.^{34,37} We assume that the increased scattering with more grain boundaries at higher GLAD creates an asymmetry in the charge carrier distribution across different energy levels, leading to a higher average energy of the carriers contributing to the thermoelectric effect.³⁸ Consequently, this presented a favorable combination for an enhanced thermoelectric power factor of up to $339 \mu\text{W}/\text{mK}^2$.

3.3. Optical Properties. This paper presents the enhanced optical transmittance of copper iodide (CuI) thin films. The optical transparency can be observed in the samples shown in Figure 4a. The transmittance values exceed 85% across the wavelength range of 560–900 nm by CuI films prepared from Cu deposited at 80° GLAD for 2 min iodination, as seen in Figure 4b. This shows a significant improvement compared to previous studies.^{1,18} The transmittance data from all other samples can be obtained from S7a,b. Also, the reported transmittance values were obtained via data processing by removing the interference fringes observed in S7c. Transmittance spectra display spectral fringes due to thin film interference. Additionally, the band gap of the CuI films was determined using Tauc's plot (can be seen from S8), yielding a value of 2.97 eV. The enhanced optical properties are attributed to the nanostructured grains with smoother surfaces formed through GLAD. Smaller and randomly distributed grains formed by GLAD reduce haziness by minimizing light scattering.^{20,39,40} The observed high transmittance in the visible range makes the demonstrated CuI thin films a compelling material for the development of next-generation transparent thermoelectric devices with enhanced efficiency and performance characteristics.

4. CONCLUSIONS

In this study, we investigated the impact of the GLAD technique on the structural, thermoelectric, and optical properties of CuI films prepared by vapor iodination. We showed that increasing GLAD to 80° led to an enhanced thermoelectric power factor of $3.39 \times 10^{-4} \text{ W}/\text{mK}^2$ at room temperature. Additionally, transmittance increased to 85% in the wavelength range of 560–900 nm. The enhanced performance in thermoelectric and optical properties is

attributed to the controlled nanoscale structural features enabled by GLAD with iodine exposure time, with the optimal results observed at an 80° deposition angle followed by 2 min of iodine vapor exposure. These results indicate that the optothermoelectric performance of CuI can be enhanced through simple and scalable manufacturing processes, making the findings highly relevant for industrial applications like transparent thermoelectric windows, which efficiently generate electricity from temperature gradients while allowing light to pass through. Moreover, CuI thin films hold immense potential for applications in on-chip cooling and power recovery in miniaturized optoelectronic devices, where they provide effective thermal management while maintaining the necessary transparency for advanced display and sensor applications.

■ ASSOCIATED CONTENT

Supporting Information

The Supporting Information is available free of charge at <https://pubs.acs.org/doi/10.1021/acsnm.4c06004>.

Information involves the variation of the thermoelectric properties of CuI grown at 0, 70, 75, and 80° GLAD about film thicknesses which changed with an exposure time of iodine; crystallite size from GIXRD data for different GLADs; transmittance spectra of CuI films grown at 30 and 60 s; the transmittance data processing by removing the interference fringes for 120 s; ImageJ software detailing for measuring grain size; and AFM topological data (PDF)

■ AUTHOR INFORMATION

Corresponding Author

Priyanka Goel – Department of Electronics and Nanoengineering, Aalto University, Espoo 00076 Aalto, Finland; orcid.org/0009-0004-7590-2954; Email: priyanka.goel@aalto.fi

Authors

Tomi Koskinen – Department of Electronics and Nanoengineering, Aalto University, Espoo 00076 Aalto, Finland; orcid.org/0000-0001-6883-4181

Ramesh Raju – Department of Electronics and Nanoengineering, Aalto University, Espoo 00076 Aalto, Finland; orcid.org/0000-0002-1802-9077

Vladimir V. Kornienko – Department of Electronics and Nanoengineering, Aalto University, Espoo 00076 Aalto, Finland; orcid.org/0000-0002-5157-3218

Weronika Wojnicka – Department of Electronics and Nanoengineering, Aalto University, Espoo 00076 Aalto, Finland

Ilkka Tittonen – Department of Electronics and Nanoengineering, Aalto University, Espoo 00076 Aalto, Finland; orcid.org/0000-0002-2985-9789

Complete contact information is available at: <https://pubs.acs.org/10.1021/acsnm.4c06004>

Author Contributions

Conceptualization, P.G. and T.K.; methodology, P.G. and T.K.; investigation, P.G., W.W., R.R., and V.V.K.; analysis, P.G. and V.V.K.; supervision, I.T.; writing-original draft, P.G.; and writing-review and editing, V.V.K., T.K., R.R., and I.T. All authors have read and agreed to the published version of the manuscript.

Funding

This work is financially supported by the Doctoral School of Electrical Engineering, Aalto University and Research Council of Finland Flagship Program PREIN.

Notes

The authors declare no competing financial interest.

ACKNOWLEDGMENTS

The authors gratefully acknowledge the support provided by the Research Council of Finland Flagship Program PREIN and the Micronova Nanofabrication Centre, Espoo, Finland, as part of the OtaNano research infrastructure at Aalto University.

ABBREVIATIONS

CuI, copper iodide; Cu, copper; GLAD, glancing angle deposition; *S*, seebeck coefficient; PF, power factor; SEM, scanning electron microscope; AFM, atomic force microscopy; GIXRD, grazing incidence X-ray diffraction; EBA, electron beam-assisted

REFERENCES

- (1) Liu, A.; Zhu, H.; Kim, M.; Kim, J.; Noh, Y. Engineering copper iodide(CuI) for multifunctional p-Type transparent semiconductors and conductors. *Adv. Sci.* **2021**, *8* (14), No. 2100546.
- (2) Lemine, A. S.; Bhadra, J.; Al-Thani, N. J.; Ahmad, Z. Promising transparent and flexible thermoelectric modules based on p-type CuI thin films—A review. *Energy Rep.* **2022**, *8*, 11607–11637.
- (3) Huang, D.; Zhao, Y.; Li, S. First-principles study of γ -CuI for p-type transparent conducting materials. *J. Phys. D: Appl. Phys.* **2012**, *45* (14), No. 145102.
- (4) Coroa, J.; Faustino, B. M.; Marques, A.; Bianchi, C.; Koskinen, T.; Juntunen, T.; Tittonen, I.; Ferreira, I. Highly transparent copper iodide thin film thermoelectric generator on a flexible substrate. *RSC Adv.* **2019**, *9*, 35384–35391.
- (5) Faustino, B. M. M.; Gomes, D.; Faria, J.; Juntunen, T.; Gasper, G.; Bianchi, C.; Almeida, A.; Tittonen, I.; Ferreira, I. CuI p-type thin films for highly transparent thermoelectric p-n modules. *Sci. Rep.* **2018**, *8* (1), No. 6867.
- (6) Wang, X.; Suwardi, A.; Lim, S.; Xu, J. Transparent flexible thin-film p–n junction thermoelectric module. *NPJ. Flexible Electron.* **2020**, *4*, No. 19.
- (7) Kaushik, D. K.; Selvaraj, M.; Ramu, S.; Subrahmanyam, A. Thermal evaporated copper iodide (CuI) thin films: A note on the disorder evaluated through the temperature dependent electrical properties. *Sol. Energy Mater. Sol. Cells.* **2017**, *165*, 52–58.
- (8) Grundmann, M. Karl, Bädeker (1877–1914) and the discovery of transparent conductive materials. *Phys. Status Solidi A* **2015**, *212* (7), 1409–1426.
- (9) Grundmann, M.; Schein, F. L.; Lorenz, M.; Böntgen, T.; Lenzner, J.; Wenckstern, H. Cuprous iodide - a p-type transparent semiconductor: history and novel applications. *Phys. Status Solidi A* **2013**, *210* (9), 1671–1703.
- (10) Weiß, A.; Goldmann, J.; Kettunen, S. Conversion of ALD CuO thin films into transparent conductive p-Type CuI thin films. *Adv. Mater. Interfaces* **2023**, *10* (3), No. 2201860.
- (11) Chinnakutti, K. K.; Panneerselvam, V.; Govindarajan, D.; Salammal, S. T. Fabrication of p-type cubic γ - CuI by solid iodination process for energy conversion and storage applications. *Mater. Today: Proc.* **2019**, *2*, 34–38.
- (12) Jamshidi, M.; Gardner, M. J. Copper(I) iodide thin films: deposition methods and hole-transporting performance. *Molecules* **2024**, *29* (8), No. 1723.
- (13) Ishibe, T.; Tomeda, A.; Watanabe, K. Methodology of thermoelectric power factor enhancement by controlling nanowire interface. *ACS Appl. Mater. Interfaces* **2018**, *10* (43), 37709–37716.
- (14) Vashae, D.; Shakouri, A. Improved thermoelectric power factor in metal-based superlattices. *Phys. Rev. Lett.* **2004**, *92* (10), No. 106103.
- (15) Mehdizadeh, D. A.; Zebarjadi, M.; He, J.; Tritt, T. M. Thermoelectric power factor: enhancement mechanisms and strategies for higher performance thermoelectric materials. *Mater. Sci. Eng., R.* **2015**, *97*, 1–22.
- (16) Yang, C.; Souchay, D.; Kneiß, M. Transparent flexible thermoelectric material based on non-toxic earth-abundant p-type copper iodide thin film. *Nat. Commun.* **2017**, *8* (1), No. 16076.
- (17) Posopa, N.; Sakulalavek, A.; Chanlek, N.; Kaewkhao, J.; Sakdanuphab, R. Room-temperature rapid synthesis of CuI thin films via liquid iodination method. *Superlattice Microstruct.* **2020**, *141*, No. 106501.
- (18) Yamada, N.; Ino, R.; Ninomiya, Y. Truly transparent p-type γ -CuI thin films with high hole mobility. *Chem. Mater.* **2016**, *28* (14), 4971–4981.
- (19) Jacob, J.; Rehman, U.; Mahmood, K. Simultaneous enhancement of Seebeck coefficient and electrical conductivity in ZnSnO by the engineering of grain boundaries using post annealing. *Phys. Lett. A* **2021**, *388*, No. 127034.
- (20) Liedtke, S.; Grüner, C.; Lotnyk, A.; Rauschenbach, B. Glancing angle deposition of sculptured thin metal films at room temperature. *Nanotechnology* **2017**, *28* (38), No. 38S604.
- (21) Lintymer, J.; Martin, N.; Chappe, J. M.; Takadom, J. Glancing angle deposition to control microstructure and roughness of chromium thin films. *Wear* **2008**, *264* (5–6), 444–449.
- (22) Hawkeye, M. M.; Brett, M. J. Glancing angle deposition: Fabrication, properties, and applications of micro- and nanostructured thin films. *J. Vac. Sci. Technol., A* **2007**, *25* (5), 1317–1335.
- (23) Santos, A. J.; Lacroix, B.; Domínguez, M.; García, R.; Martin, N.; Morales, F. M. Controlled grain-size thermo-chromic VO₂ coatings by the fast oxidation of sputtered vanadium or vanadium oxide films deposited at glancing angles. *Surf. Interfaces* **2021**, *27*, No. 101581.
- (24) Klochko, P. N.; Zhadan, O. D.; Klepikova, S. K.; Petrushenko, I. S.; Kopach, R. V.; Khrypunov, S. G.; Lyubov, M. V.; Dukarov, V. S.; Khrypunova, L. A. Semi-transparent copper iodide thin films on flexible substrates as p-type thermoelectrics for a wearable thermoelectric generator. *Thin Solid Films* **2019**, *683*, 34–41.
- (25) Herrick, C. S. Oxygen-inhibited grain growth in thin films of semiconducting cuprous iodide. *Nature* **1966**, *211*, 958–959.
- (26) Wang, J.; Li, J.; Li, S. S. Native p -type transparent conductive CuI via intrinsic defects. *J. Appl. Phys.* **2011**, *110* (5), No. 054907.
- (27) Ruoho, M.; Juntunen, T.; Tittonen, I. Large-area thermoelectric high-aspect-ratio nanostructures by atomic layer deposition. *Nanotechnology* **2016**, *27* (35), No. 355403.
- (28) Sirimanne, P. M.; Rusop, M.; Shirata, T.; Soga, T.; Jimbo, T. Characterization of CuI thin films prepared by different techniques. *Mater. Chem. Phys.* **2003**, *80* (2), 461–465.
- (29) Alam, J.; Su, X.; Kuan, H. C.; Vahid, S. A.; Zuber, K.; Meng, Q.; Meng, F.; Losic, D.; Ma, J. Preparation, morphology and thermo-

electric performance of PEDOT/CuI nanocomposites. *Funct. Compos. Mater.* **2023**, *4* (1), No. 9.

(30) Yude, Y.; Boysen, H.; Schulz, H. Neutron powder investigation of CuI*. *Z. Kristallogr.* **1990**, *191* (1–2), 79–91.

(31) Monshi, A.; Foroughi, M. R.; Monshi, M. R. Modified Scherrer equation to estimate more accurately nano-crystallite size using XRD. *World J. Nano Sci. Eng.* **2012**, *02* (3), 154–160.

(32) Vick, D.; Friedrich, L. J.; Dew, S. K. Self-shadowing and surface diffusion effects in obliquely deposited thin films. *Thin Solid Films* **1999**, *339* (1–2), 88–94.

(33) Vora-ud, A.; Chaarmart, K.; Kasemsin, W.; Boonkirdram, S.; Seetawan, T. Transparent thermoelectric properties of copper iodide thin films. *Phys. B* **2022**, *625*, No. 413527.

(34) Lohani, K.; Nautiyal, H.; Ataollahi, N.; Maji, K.; Guilmeau, E.; Scardi, P. Effects of grain size on the thermoelectric properties of Cu₂SnS₃: an experimental and first-principles study. *ACS Appl. Energy Mater.* **2021**, *4* (11), 12604–12612.

(35) Amin, N.; Ali, A.; Mahmood, K.; Basha, B.; Al-Buriah, M. S.; Alrowaili, Z. A.; Nawaz, I.; Waheed, H.; Rasool, S.; Rasheed, Z.; Anwar, H.; Saleem, M.; Ali, M. Y.; Javaid, K. Annealing-induced transformation of structural and optical parameters of transparent γ -CuI thin films with superior thermoelectric performance. *Ceram. Int.* **2024**, *50* (19), 36884–36891.

(36) Ali, H. T.; Amami, M.; Rehman, U.; Mahmood, K.; Ikram, S.; Ali, A.; Amin, N.; Javaid, K.; Arshad, I. M. Investigating the thermoelectric power generation performance of ZnCuO: A p-type mixed-metal oxide system. *J. Phys. Chem. Solids* **2022**, *163*, No. 110535.

(37) Bachmann, M.; Czerner, M.; Heiliger, C. Ineffectiveness of energy filtering at grain boundaries for thermoelectric materials. *Phys. Rev. B* **2012**, *86* (11), No. 115320.

(38) Mahmood, K.; Jacob, J.; Zahra, R.; Ail, A.; Rehman, U.; Ashfaq, A.; Ahmed, W.; Amin, N.; Arshad, M. I.; Javaid, K.; Ikram, S.; Ajaz un Nabi, M.; Hussain, S.; Feng, Y. Thermoelectric properties of Zn₂GeO₄ nano-crystals grown on ITO and Au coated Si substrates by thermal evaporation. *Ceram. Int.* **2019**, *45* (15), 18333–18337.

(39) Charles, C.; Martin, N.; Devel, M.; Ollitrault, J.; Billard, A. Correlation between structural and optical properties of WO₃ thin films sputter deposited by glancing angle deposition. *Thin Solid Films* **2013**, *534*, 275–281.

(40) Shahidi, M. M.; Rezagholipour, D. H.; Ehsani, M. H.; Ghazi, M. E. Effect of GLAD technique on optical and electrical properties of SnO₂/Ag/SnO₂ structure. *Infrared Phys. Technol.* **2020**, *106*, No. 103263.